Selenoether Macrocyclic Chemistry: Syntheses, NMR Studies, Redox Properties, and Single-Crystal Structures of $[M([16]aneSe_4)](PF_6)_2 \cdot 2MeCN$ (M = Pd, Pt; [16]aneSe$_4$ = 1,5,9,13-Tetraselenacyclohexadecane)

Neil R. Champness,[†] Paul F. Kelly,[†] William Levason,[†] Gillian Reid,*[,†] Alexandra M. Z. Slawin,[‡] and David J. Williams[‡]

Departments of Chemistry, University of Southampton, Highfield, Southampton SO9 5NH, England, and Imperial College of Science, Technology and Medicine, South Kensington, London SW7 2AY, England

Received April 27, 1994[⊗]

Reaction of MCl_2 (M = Pd, Pt) with 1 molar equiv of [16]aneSe$_4$ in refluxing MeCN solution in the presence of $TlPF_6$ affords the complexes $[M([16]aneSe_4)](PF_6)_2$ in high yield. $[Pd([16]aneSe_4)](PF_6)_2 \cdot 2MeCN$ crystallizes in the monoclinic space group $P2_1/c$ with a = 10.184(4) Å, b = 10.673(4) Å, c = 13.960(7) Å, β = 98.01(4)°, V = 1502.6 Å^3, Z = 2, and $F(000)$ = 917. The structure shows the Pd^{II} ion on a center of symmetry at (0, 0, 0), coordinated to a precisely square planar arrangement of the four selenoether donor atoms, with the macrocycle adopting an *up,up,down,down* configuration, Pd–Se = 2.435(2), 2.428(1) Å. $[Pt([16]aneSe_4)](PF_6)_2 \cdot 2MeCN$ is isomorphous with its Pd^{II} analogue, giving a = 10.200(7) Å, b = 10.609(6) Å, c = 14.045(8) Å, β = 98.90(2)°, V = 1501.6 Å^3, Z = 2, $F(000)$ = 984, and Pt–Se = 2.420(3), 2.417(3) Å. Variable-temperature ^{77}Se and ^{195}Pt NMR studies are described which reveal the occurrence of a dynamic process in solution for $[M([16]aneSe_4)]^{2+}$, involving interconversion of invertomers. The bis-bidentate model complexes $[M(MeSeCH_2CH_2CH_2SeMe)_2](PF_6)_2$ have also been prepared by reaction MCl_2 with 2 molar equiv of $MeSeCH_2CH_2CH_2SeMe$ in refluxing MeCN in the presence of $TlPF_6$. Variable-temperature ^{77}Se and ^{195}Pt NMR spectroscopic studies on these complexes are compared with those of the macrocyclic tetraselenoether complexes. Cyclic voltammetry of $[M([16]aneSe_4)](PF_6)_2$ in MeCN solution shows no oxidative activity. An irreversible reduction is seen for each complex at E_{pc} = −0.90 V for M = Pd and E_{pc} = −1.64 V *vs* Fc/Fc$^+$ for M = Pt, at a scan rate of 200 mV s^{-1}.

Introduction

Since the discovery of crown ethers by Pedersen in 1967, interest in macrocyclic ligand chemistry has escalated.[1] In particular, the chemistry of thioether macrocycles has received considerable attention over the past decade. These have proved to be very good ligands for a wide range of d- and p-block ions.[2] An important feature of these systems is their ability to adopt unpredictable geometries and stabilize unusual oxidation states—sometimes at the expense of the normal oxidation states. For example, the Au^I center in $[Au([9]aneS_3)_2]^+$ is apparently destabilized by the trithia macrocycles which prefer the highly unusual mononuclear Au^{II} state. Hence the complex cation $[Au([9]andS_3)_2]^{2+}$ is readily isolated.[3]

Despite this rich coordination chemistry exhibited by thioether macrocycles, the effect of incorporating heavier selenoether donor atoms into a macrocyclic configuration has remained a poorly studied area.[4–6] This is surprising since selenoethers display two major advantages over their thia counterparts: first, they are better σ-donors and, as such, should offer more powerful ligation to transition metal ions; second, ^{77}Se NMR spectroscopy (I = $^1/_2$, 7.58%, D_c = 2.98) is an excellent probe with which to monitor structures in solution. To date, Pinto and co-workers, who reported the syntheses of a series of selenacrowns, including [14]aneSe$_4$, [16]aneSe$_4$, and [24]aneSe$_6$, are the only major contributors to this area.[4] They have also alluded to the potential of these compounds as ligands through the synthesis of Cu^I, Cu^{II}, and Hg^{II} complexes incorporating [16]aneSe$_4$.[5]

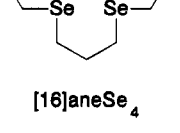

[16]aneSe$_4$

As part of our work aimed at establishing the nature of selenoether to transition metal bonding, we recently reported the synthesis and structure of *trans*-$[RhCl_2([16]aneSe_4)]^+$. This

[†] University of Southampton.
[‡] Imperial College of Science, Technology and Medicine.
[⊗] Abstract published in *Advance ACS Abstracts,* January 1, 1995.

(1) *Coordination Chemistry of Macrocyclic Compounds*; Melson, G. A., Ed.; Plenum: New York, 1979. *The Chemistry of Macrocyclic Ligand Complexes*; Lindoy, L. F., Ed.; Cambridge University Press: Cambridge, U.K., 1989.
(2) Schröder; M. *Pure Appl. Chem.* 1987, *60*, 517; Blake, A. J.; Schröder, M. *Adv. Inorg. Chem.* **1990**, *35*, 1. Cooper, S. R. *Acc. Chem. Res.* **1988**, *21*, 141. Cooper, S. R.; Rawle, S. C. *Struct. Bonding (Berlin)* **1990**, *72*, 1.
(3) Blake, A. J.; Gould, R. O.; Greig, J. A.; Holder; A. J.; Hyde, T. I.; Schröder; M. *J. Chem. Soc., Chem. Commun.* **1989**, 876. Blake, A. J.; Greig, J. A.; Holder, A. J.; Hyde, T. I.; Schröder, M. *Angew. Chem., Int. Ed. Engl.* **1990**, *29*, 197. Blake, A. J.; Gould, R. O.; Radek, C.; Reid, G.; Taylor, A.; Schröder, M. In *The Chemistry of the Copper and Zinc Triads*; Welch, A. J.; Chapman, S. K., Eds.; The Royal Society of Chemistry: London, 1993, p 95.
(4) Batchelor, R. J.; Einstein, F. W. B.; Gay, I. D.; Gu, J.-H.; Johnston, B. D.; Pinto, B. M. *J. Am. Chem. Soc.* **1989**, *111*, 6582.
(5) Batchelor, R. J.; Einstein, F. W. B.; Gay, I. D.; Gu, J.-H.; Pinto, B. M.; Zhou, X.-M. *J. Am. Chem. Soc.* **1990**, *112*, 3706. Batchelor, R. J.; Einstein, F. W. B.; Gay, I. D.; Gu, J.-H.; Pinto, B. M. *J. Organomet. Chem.* **1991**, *411*, 147.
(6) Kumagai, T.; Akabori, S. *Chem. Lett.* **1989**, 1667. Muralidharan, S.; Hojjati, M.; Firestone, M.; Freiser, H. *J. Org. Chem.* **1989**, *54*, 393.

0020-1669/95/1334-0651$09.00/0

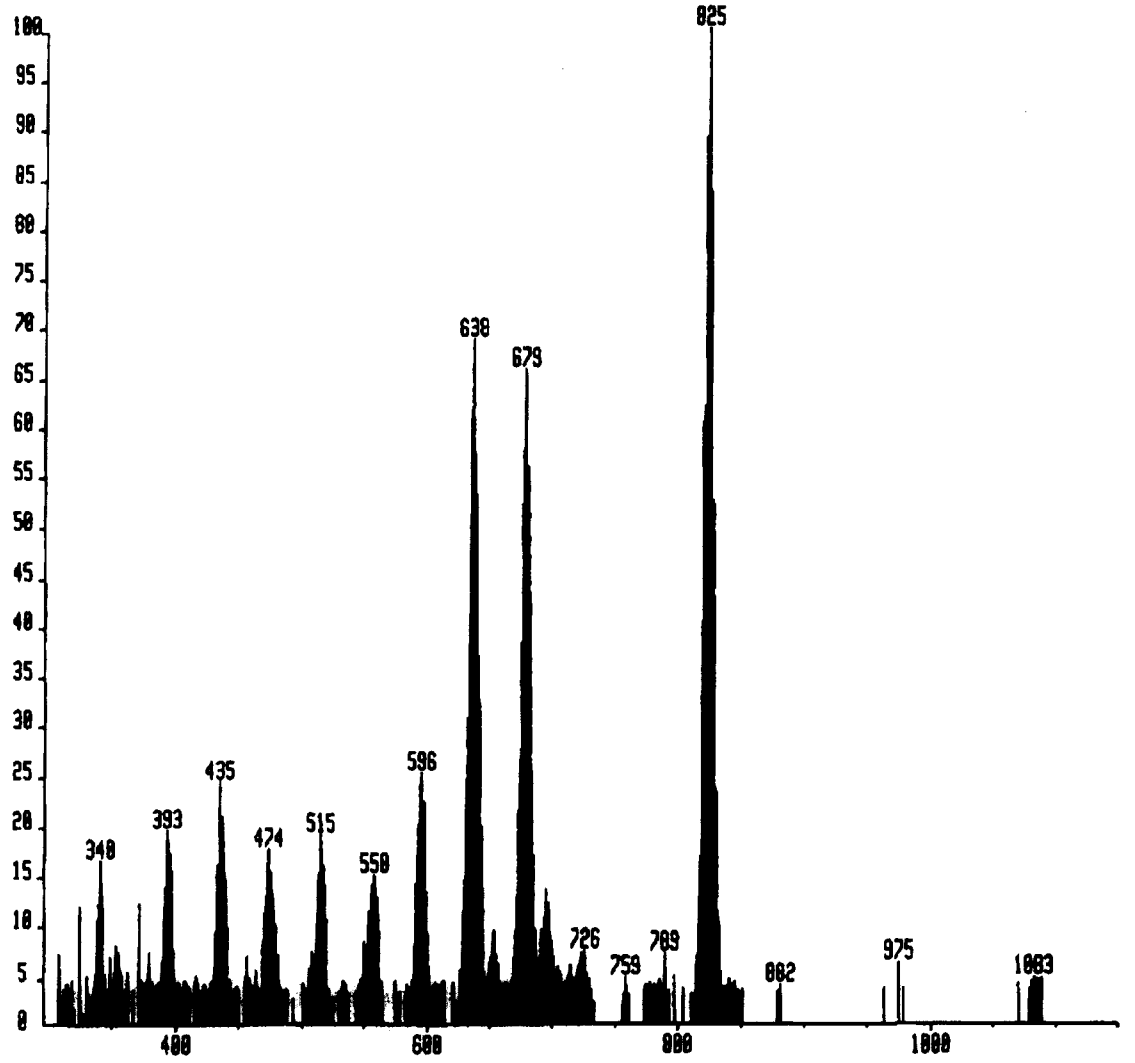

Figure 1. FAB mass spectrum (3-NOBA) of $[Pt([16]aneSe_4)](PF_6)_2$.

cation adopts an *up,up,down,down* configuration at the Se donors; Rh−Se = 2.348(3), Rh−Cl = 2.339(2) Å.[7] We now report the syntheses, single-crystal X-ray structures, multinuclear NMR (^1H, ^{13}C, ^{77}Se, ^{195}Pt) spectroscopy, and redox properties of $[M([16]aneSe_4)](PF_6)_2 \cdot 2MeCN$ (M = Pd, Pt). The syntheses and NMR spectroscopic data for the acyclic model systems $[M(MeSeCH_2CH_2CH_2SeMe)_2](PF_6)_2$ (M = Pd, Pt) are also reported.

Results and Discussion

The tetraselena crown $[16]aneSe_4$ (1,5,9,13-tetraselenacyclohexadecane) was prepared through the [2 + 2] cyclization of the disodium salt of 1,3-diselenapropane with 1,3-dibromopropane using the method reported by Pinto *et al.*[4] Reaction of $PdCl_2$ with 1 molar equiv of $[16]aneSe_4$ and 2 molar equiv of $TlPF_6$ in refluxing MeCN for *ca.* 2 h affords a yellow solution together with a TlCl precipitate. After filtration, the volume of solvent was reduced *in vacuo* to *ca.* 2 mL. Slow diffusion of Et_2O into this solution yields yellow crystals of $[Pd([16]aneSe_4)](PF_6)_2 \cdot 2MeCN$. Similar reaction with $PtCl_2$ yields colorless crystals of $[Pt([16]aneSe_4)](PF_6)_2 \cdot 2MeCN$. The IR spectra of these products confirm the presence of coordinated $[16]aneSe_4$ and PF_6^- counterions. The FAB mass spectra of the complexes exhibit peaks with the correct isotopic distributions based on ^{195}Pt, ^{106}Pd, and ^{79}Se for $[M([16]aneSe_4)PF_6]^+$ and $[M([16]aneSe_4)]^+$, respectively (*m/z*: M = Pd, M^+ = 736, 591; M = Pt, M^+ = 825, 679). Figure 1 shows the FAB mass spectrum obtained for $[Pt([16]aneSe_4)](PF_6)_2$. In addition to the peaks listed above, the spectrum clearly shows fragmentation peaks consistent with successive loss of $(CH_2)_3$ linkages and of selenium atoms from the macrocyclic framework. This fragmentation pattern is not observed for the analogous tetrathia macrocyclic complex, $[Pt([16]aneS_4)]^{2+}$,[8] indicating that Se−C bonds are considerably weaker than S−C bonds under the conditions employed for FAB mass spectrometry. This is consistent with the observation that elimination of alkyl linkages can occur in selenoether complexes and has been noted before in the EI mass spectra of dithio- and diselenoether ligands.[9]

Crystals suitable for single-crystal X-ray analyses were obtained for both complexes by slow diffusion of Et_2O into a solutions of the complexes in MeCN. Single-crystal X-ray structure determinations of $[M([16]aneSe_4)](PF_6)_2 \cdot 2MeCN$ (M = Pd, Pt) show that these species are isomorphous, with a square planar arrangement of the four selenoether donors around the central metal ion (which lies on a center of symmetry) in an *endocyclic* arrangement (Figures 2 and 3): Pd−Se(1) = 2.435(2), Pd−Se(5) = 2.428(1) Å; Pt−Se(1) = 2.420(3), Pt−Se(5) = 2.417(3) Å. The macrocycle adopts an *up,up,down,down* configuration in each case, similar to that seen in *trans*-$[RhCl_2$-

(7) Kelly, P. F.; Levason, W.; Reid, G.; Williams, D. J. *J. Chem. Soc., Chem. Commun.* **1993**, 1716.

(8) Blake, A. J.; Holder, A. J.; Reid, G.; Schröder, M. *J. Chem. Soc., Dalton Trans.* **1994**, 627.

(9) For examples see: Hope, E. G.; Levason, W. *Coord. Chem. Rev.* **1993**, *122*, 109.

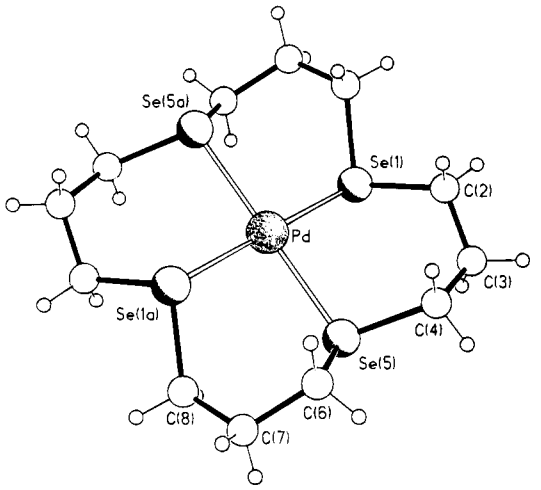

Figure 2. View of the structure of $[Pd([16]aneSe_4)]^{2+}$ with numbering scheme adopted.

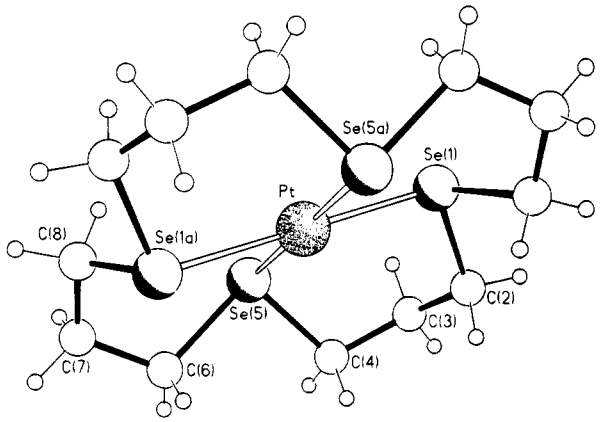

Figure 3. View of the structure of $[Pt([16]aneSe_4)]^{2+}$ with numbering scheme adopted.

$([16]aneSe_4)]^+$.[7] The metal ions lie precisely in the Se_4 coordination plane. A similar structure has also been observed for the thioether macrocyclic complex $[Pd([16]aneS_4)]^{2+}$, Pd–S = 2.303(10), 2.304(10) Å, suggesting that the cavities available for [16]aneSe$_4$ and [16]aneS$_4$ are very similar in size.[10] The longer Pd–donor atom bond lengths in the title complexes are in accord with the larger radius of Se over S. The Se–M–Se angles in the title complexes are all within 1.1° of 90 or 180°, indicating the good size match between the crown and the metal ion radii. Two non-coordinating MeCN solvent molecules were found to be associated with each M^{2+} cation during refinement. The structural parameters for $[Pt([16]aneSe_4)]^{2+}$ are rather less accurate than those for the Pd(II) analogue. This is because of the truncated data set obtained for the Pt(II) complex (see Experimental Section) and the resultant limited ratio of observations to variable parameters. However, the data were sufficient to adequately establish the molecular geometry.

Study of the packing of the molecules in the crystals reveals only one pair of notable short contacts. These involve a pseudoaxial approach of pairs of centrosymmetrically related F atoms to the metal centers. The F···Pt and F···Pd distances are 3.39 and 3.24 Å, respectively. There are no close contacts to the MeCN solvent molecules.

The solution structures of the selenoether macrocyclic complexes were probed by NMR spectroscopy (^{13}C, ^{77}Se, ^{195}Pt). The $^{13}C\{^1H\}$ NMR spectra of $[M([16]aneSe_4)]^{2+}$ (M = Pd, Pt) show several resonances in the range expected for Se–C linkages (*ca.* 27–33 ppm) and several others around 23 ppm corresponding to the methylene groups at the center of the C_3 linkages. In each case, the total number of carbon resonances suggests that more than one form of the cation $[M([16]aneSe_4)]^{2+}$ is present. Four distinct invertomers are possible for square planar $[M([16]aneSe_4)]^{2+}$ depending upon the orientation of the Se lone pairs. It is likely that one of these (*up,up, up,down*) may be rather less stable than the other three (*up,up, up,up*; *up,up,down,down*; *up,down,up,down*) due to ring strain.

Free [16]aneSe$_4$ shows a single resonance in the ^{77}Se solution NMR spectrum at +157 ppm.[4] At 298 K in MeCN or Me_2CO solution, the ^{77}Se NMR spectrum of $[Pd([16]aneSe_4)](PF_6)_2$ shows two resonances at 196 and 153 ppm consistent with the presence of at least two invertomers in solution under these conditions. Cooling to 210 K in Me_2CO solution gives a single, relatively broad resonance at 203 ppm. Similar behavior is observed for $[Pt([16]aneSe_4)](PF_6)_2$ (Figure 4). In MeCN solution at 300 K, the ^{77}Se NMR spectrum shows two resonances at 187 and 147 ppm. These signals are not shifted significantly in $MeNO_2$ or Me_2CO solution. Cooling to 260 K in MeCN resolves the upfield signal to give three ^{77}Se resonances at 189, 146, and 141 ppm. Further cooling (Me_2CO) to 185 K gives a single resonance at 187 ppm.

^{195}Pt NMR spectra were also recorded for $[Pt([16]aneSe_4)]^{2+}$. In MeCN solution at 300 K, the ^{195}Pt NMR spectrum shows three resonances at −4568, −4587, and −4676 ppm. At 280 K in Me_2CO, the major species occurs at −4716 ppm with two minor species at −4614 and −4594 ppm. Cooling to 210 K results in a single, relatively broad resonance at −4750 ppm (line width at half-height *ca.* 240 Hz). We have not been able to resolve any ^{195}Pt–^{77}Se coupling in these spectra even at 185 K in either the ^{77}Se or the ^{195}Pt NMR spectra, since the lines are still relatively broad. These results indicate that $^1J_{PtSe}$ is less than the line widths, *ca.* 200 Hz. (Note: Since acceptance of this paper, working in acetone/$CDCl_3$ at 300 K, we observed the Pt–Se couplings, giving $^1J_{PtSe}$ *ca.* 90 Hz. Upon cooling, these couplings were lost due to broadening of the lines.) Very few $^1J_{PtSe}$ coupling constants for *trans* Se–Pt–Se units have been reported; however, the data available indicate that they are smaller than for *trans* Se–Pt–Cl and tend to be sensitive to the substituents at selenium.[11] These results are indicative of some dynamic process occurring in solution over the temperature range which we are investigating. This behavior contrasts with that of the octahedral d^6 Rh^{III} cation *trans*-$[RhCl_2([16]aneSe_4)]^+$, which shows only one signal in the ^{77}Se NMR spectrum, at δ +160, consistent with the solid-state structure being retained in solution. In this case, the doublet coupling to ^{103}Rh ($I = {}^1/_2$, 100%) is also apparent, giving $^1J_{RhSe}$ *ca.* 30 Hz.[7]

We were suspicious that the ^{77}Se NMR resonance at 147 ppm for $[Pt([16]aneSe_4)]^{2+}$ was due to uncoordinated Se donor atoms of the macrocycle. However, we have been unable to find species of the form $[Pt(\eta^2\text{-}[16]aneSe_4)(solvent)_2]^{2+}$ or $[Pt(\eta^2\text{-}[16]aneSe_4)Cl_2]$ in the ^{195}Pt NMR spectrum. Together with the observation that the ^{77}Se and ^{195}Pt NMR signals do not shift significantly with solvent, this strongly suggests that the signals are due to tetraligated macrocyclic species as originally expected.

In an attempt to elucidate the nature of the fluxional process occurring in the Pd^{II} and Pt^{II} tetraselena crown systems and to

(10) Reid, G. Ph.D. Thesis, University of Edinburgh, 1989. Blake, A. J.; Reid, G.; Schröder, M. Unpublished results.

(11) Hope, E. G.; Levason, W.; Murray, S. G.; Marshall, G. L. *J. Chem. Soc., Dalton Trans.* **1985**, 2185. McFarlane, W. *J. Chem. Soc., Dalton Trans.* **1974**, 324. Chadha, R. K.; Chehayber, J. M.; Drake, J. E. *Inorg. Chem.* **1986**, *25*, 611.

(12) Gulliver, D. G.; Hope, E. G.; Levason, W.; Murray, S. G.; Marshall, G. L. *J. Chem. Soc., Dalton Trans.* **1985**, 1265.

(13) Kemmitt, T.; Levason, W.; Webster, M. *Inorg. Chem.* **1989**, *28*, 697.

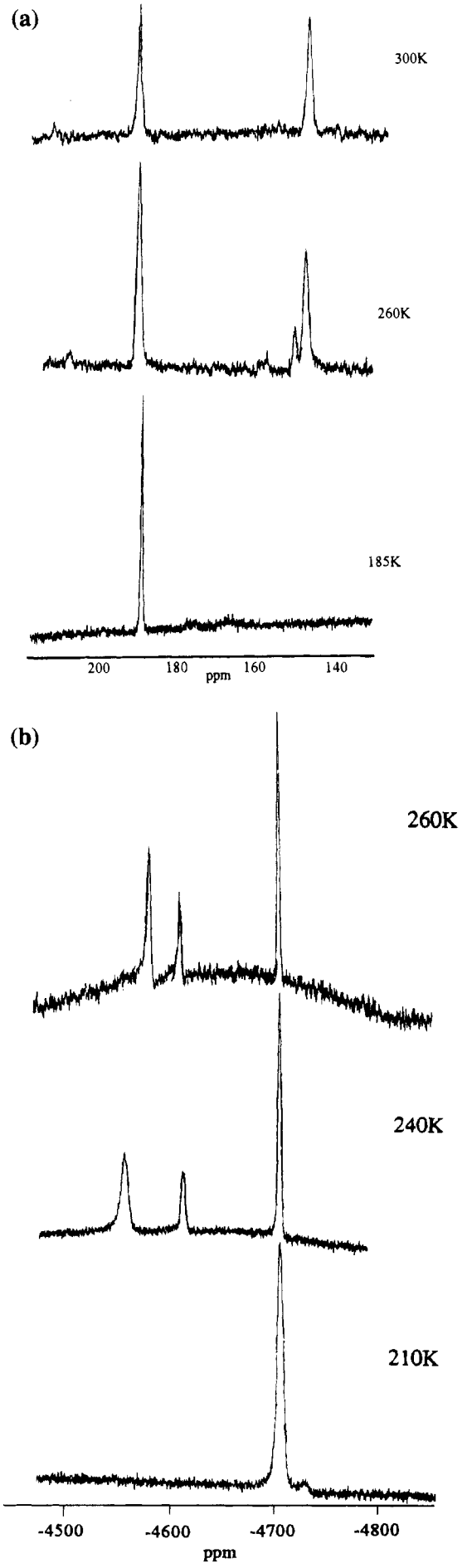

Figure 4. Variable-temperature ^{77}Se (a) and ^{195}Pt (b) NMR spectra of $[Pt([16]aneSe_4)]^{2+}$ in $(CD_3)_2CO$ solution.

establish whether it is due to ring effects, the acyclic bis-bidentate selenoether complexes $[M(MeSeCH_2CH_2CH_2SeMe)_2](PF_6)_2$ (M = Pd, Pt) were prepared. These were obtained by reaction of MCl_2 with 2 molar equiv of $MeSeCH_2CH_2CH_2SeMe$ in refluxing MeCN in the presence of 2 molar equiv of $TlPF_6$ to abstract halide. The formulation of the complexes was confirmed by microanalyses, IR, UV/visible, and ^1H and $\{^1H\}^{13}C$ NMR spectroscopy, and FAB mass spectrometry. ^{77}Se NMR studies on $[Pd(MeSeCH_2CH_2CH_2SeMe)_2](PF_6)_2$ in Me_2CO solution reveal a single, broad resonance at 132 ppm at 300 K. Upon cooling to 255 K, four distinct resonances become apparent at 135, 132, 128, and 118 ppm. Further cooling to 200 K results in a single resonance at 124 ppm. In contrast, the ^{77}Se NMR spectrum of $[Pt(MeSeCH_2CH_2CH_2SeMe)_2](PF_6)_2$ in Me_2CO solution at 320 K shows two broadened resonances at 128 and 127 ppm. Cooling to 225 K gives three resonances at 125, 124, and 122 ppm. The ^{195}Pt NMR spectrum of this complex cation shows a major species at −4677 ppm and two minor species at −4663 and −4657 ppm at 320 K. The ^{195}Pt NMR spectrum does not change significantly upon cooling to 185 K, and the signals remain relatively broad, making determination of the Pt−Se couplings difficult. These results suggest that $[Pd(MeSeCH_2CH_2CH_2SeMe)_2]^{2+}$ is undergoing faster inversion at selenium on the NMR time scale within the temperature range investigated compared to the Pt^{II} analogue. This observation is not unusual.[14]

Addition of excess Cl^- anion to MeCN solutions of $[M(MeSeCH_2CH_2CH_2SeMe)_2](PF_6)_2$ (M = Pd, Pt) resulted in a color change to golden yellow and precipitation of a yellow solid in each case. ^{77}Se and ^{195}Pt NMR studies in dmso solution indicate the presence of free $MeSeCH_2CH_2CH_2SeMe$ ligand ($\delta(^{77}Se) = 68$) together with the known species $MCl_2(MeSeCH_2CH_2CH_2SeMe)$ (M = Pd, $\delta(^{77}Se) = 198$; M = Pt, $\delta(^{77}Se) = 168$ ($J_{PtSe} = 500$ Hz) and 185 ($J_{PtSe} = 510$ Hz).[11] These results confirm that addition of Cl^- results in loss of one of the bidentate selenoether ligands and uptake of two Cl^- ligands to give $MCl_2(MeSeCH_2CH_2CH_2SeMe)$, incorporating a Cl_2Se_2 donor set around the central metal ion. Both the meso and DL isomeric forms are evident for the Pt^{II} complex, whereas $PdCl_2(MeSeCH_2CH_2CH_2SeMe)$ is known to be inverting rapidly at room temperature, showing only a single resonance.[11]

Excess Cl^- anion was also added to a solution of $[Pt([16]aneSe_4)](PF_6)_2$ in MeCN. This resulted in almost immediate precipitation of a yellow solid. Attempts to identify this product were hampered by its poor solubility in most solvents. However, it partially redissolved in dmso solution, enabling a ^{77}Se NMR spectrum to be recorded. This shows a resonance at δ +176 with $^1J_{PtSe}$ *ca.* 196 Hz. A further very weak resonance at δ +156 was assigned to a small quantity of free $[16]aneSe_4$ in solution. The ^{195}Pt NMR spectrum shows a single resonance at −4503 ppm, corresponding to a small downfield shift with respect to the $[Pt([16]aneSe_4)]^{2+}$ starting material. It is however considerably upfield from that of a Cl_2Se_2 donor set at Pt^{II}, which would resonate in the range −3400 to −3700 ppm.[11,13] Thus, the resonances corresponding to the original $[Pt([16]aneSe_4)]^{2+}$ species are no longer evident, confirming conversion to a new product, probably still involving Se_4 coordination, possibly with an apical Cl^- ligand giving a five-coordinate platinum(II) species. Further experiments are necessary to confirm this.

Cyclic voltammetric measurements on $[M([16]aneSe_4)](PF_6)_2$ (M = Pd, Pt) in MeCN solution (0.1 M $^nBu_4NBF_4$ supporting electrolyte) show an irreversible reduction at $E_{pc} = -0.90$ and −1.64 V vs Fc/Fc^+, respectively, at a scan rate of 200 mV s^{-1}. No oxidative activity is seen under these conditions up to +2.0

(14) Abel, E. W.; Bhargava, S. K.; Orrell, K. G. *Prog. Inorg. Chem.* **1984**, *32*, 1. Orrell, K. G. *Coord. Chem. Rev.* **1989**, *96*, 1.

Table 1. X-ray Data Collection Parameters for $[M([16]aneSe_4)](PF_6)_2 \cdot 2MeCN$ (M = Pd, Pt)

	M = Pd	M = Pt
formula	$C_{12}H_{24}Se_4Pd(PF_6)_2 \cdot 2MeCN$	$C_{12}H_{24}Se_4Pt(PF_6)_2 \cdot 2MeCN$
mol wt	960.9	1051.3
color, morphology	yellow blocks	colorless blocks
crystal size/mm	0.23 × 0.33 × 0.66	0.20 × 0.20 × 0.50
crystal system	monoclinic	monoclinic
a/Å	10.184(4)	10.200(7)
b/Å	10.673(4)	10.609(6)
c/Å	13.960(7)	14.045(8)
β/deg	98.01(4)	98.90(2)
V/Å^3	1502.6	1501.6
space group	$P2_1/c$	$P2_1/c$
Z	2	2
D_{calc}/g·cm^{-3}	2.124	2.325
λ/Å	0.710 73 (Mo)	0.710 73 (Mo)
μ/cm^{-1}	56.4	97.1
$F(000)$	917	984
transm factors: max, min	0.2549, 0.4902	0.1868, 0.4982
no. of unique data	2644	1108
no. of obsd data with $F > 3\sigma(F)$	1988	789
scan type	ω	ω
2θ range/deg	3−50	3−45
final $\Delta\rho$/e Å^{-3}	1.32	0.81
final Δ/σ	0.050	0.192
$R = \Sigma(F_o - F_c)/\Sigma F_o$	5.35	5.59
R_w	5.01	5.06
temp/K	293	293

V. This is similar to the behavior of the tetrathia analogues $[M([16]aneS_4)]^{2+}$ (M = Pd, Pt), which show irreversible reductions at $E_{pc} = -0.88$ and -1.50 V *vs* Fc/Fc$^+$, respectively. These data indicate that the thioether and selenoether ligands exhibit similar donor strengths. On the basis of coulometric measurements, for $[M([16]aneS_4)]^{2+}$ these reductions were tentatively assigned to $M^{II/I}$ redox couples, involving rapid quenching of the reactive M^I species.[8,10]

These results confirm that a range of transition metal ions will readily insert into the cavity of the tetraselena crown [16]-aneSe$_4$ to yield complexes with a square planar Se$_4$ donor set. From the single-crystal X-ray studies, the *up,up,down,down* form appears to be the preferred invertomer in the solid state for these complexes. However, while $[RhCl_2([16]aneSe_4)]^+$ appears to retain its solid state configuration in solution, the d^8 cations $[M([16]aneSe_4)]^{2+}$ (M = Pd, Pt) undergo inversion in solution between 185 and 300 K. We hope to use 2-D NMR spectroscopy and molecular mechanics/dynamics calculations to identify the exact origin of the dynamic processes occurring in solution for the macrocyclic selenoether cations $[M([16]aneSe_4)]^{2+}$.

Experimental Section

Infrared spectra were measured as KBr or CsI disks or as Nujol mulls using a Perkin-Elmer 983 spectrometer over the range 200−4000 cm^{-1}. Mass spectra were run by electron impact or fast-atom bombardment (FAB) using 3-NOBA (3-nitrobenzyl alcohol) as matrix on a VG Analytical 70-250-SE normal-geometry double-focusing mass spectrometer. Solution UV/visible spectra were recorded in 1 cm path length quartz cells using a Perkin-Elmer Lambda 19 spectrophotometer. ^{1}H NMR spectra were recorded using a Bruker AM300 spectrometer. $^{13}C\{^1H\}$ NMR spectra were recorded using a Bruker AM360 spectrometer operating at 90.53 MHz. ^{77}Se NMR spectra were recorded using a Bruker AM360 spectrometer operating at 68.68 MHz and are referenced to neat Me_2Se ($\delta = 0$). ^{195}Pt NMR spectra were run using 10 mm diameter tubes containing 10−15% deuterated solvent or a 5 mm insert tube of D_2O as a lock, on a Bruker AM360 spectrometer operating at 77.4 MHz and are referenced against a solution of Na_2PtCl_6 in H_2O ($\delta = 0$). Microanalyses were performed by the Imperial College microanalytical service. Cyclic voltammetric experiments were performed using an EG&G Princeton Applied Research Model 362 scanning potentiostat with 0.1 M $^nBu_4NBF_4$ supporting electrolyte, using a double platinum electrode as working and auxiliary electrode and a Ag/AgCl reference electrode. All potentials are quoted versus ferrocene/ferrocenium (Fc/Fc$^+$). [16]aneSe$_4$[4] and $MeSeCH_2CH_2CH_2SeMe$[15] were prepared according to literature methods.

(a) Synthesis of $[Pd([16]aneSe_4)](PF_6)_2$. $PdCl_2$ (16 mg, 0.09 mmol), [16]aneSe$_4$ (43 mg, 0.09 mmol), and $TlPF_6$ (62 mg, 0.18 mmol) were refluxed in MeCN (30 mL) under a dinitrogen atmosphere for 2 h to give a yellow solution and white precipitate. Consumption of all the [16]aneSe$_4$ after this period was confirmed by TLC. The solution was then filtered to remove the TlCl and reduced to *ca.* 2 mL *in vacuo*. The product was isolated as large well-formed yellow crystals by slow diffusion of Et_2O into the MeCN solution. Anal. Calcd for $C_{12}H_{24}F_{12}P_2PdSe_4$: C, 16.3; H, 2.45. Found: C, 16.4; H, 2.70. FAB mass spectrum (3-NOBA matrix), *m/z*: found $M^+ = 736$ and 591; calculated for $[Pd([16]aneSe_4)PF_6]^+$ $M^+ = 737$, $[Pd([16]aneSe_4)]^+$ $M^+ = 592$. UV/visible spectrum (MeCN solution): $\lambda_{max} = 310$ nm ($\epsilon_{mol} = 19\,500$ dm^3 mol^{-1} cm^{-1}). $^{13}C\{^1H\}$ NMR spectrum (90.53 MHz, $(CD_3)_2CO$, 300 K): 32.7, 31.5, 31.3, 27.1, 23.8 ppm. $^{77}Se\{^1H\}$ NMR spectrum: (68.68 MHz, MeCN, 300 K) 196, 153 ppm; (Me_2CO, 210K) 210 ppm. IR spectrum (Nujol mull): 2725 m, 1300 m, 1261 m, 1228 w, 1154, 1076 w, 839 vs, b, 557 vs cm^{-1}.

Table 2. Atomic Coordinates (×10^4) and Equivalent Isotropic Displacement Coefficients (Å^2 × 10^3) for $[Pd([16]aneSe_4)]^{2+}$

	x	*y*	*z*	*U*(eq)[a]
Pd	0	0	0	32(1)
Se(1)	−818(1)	1799(1)	−979(1)	42(1)
C(2)	−1362(9)	3047(9)	−87(7)	52(3)
C(3)	−256(10)	3573(9)	618(7)	58(4)
C(4)	289(10)	2701(9)	1421(7)	51(3)
Se(5)	1458(1)	1396(1)	1029(1)	43(1)
C(6)	1665(11)	585(11)	2291(6)	60(4)
C(7)	2711(10)	−477(11)	2344(7)	61(4)
C(8)	2632(9)	−1324(10)	1479(7)	54(3)
P(1)	3080(3)	−70(3)	8060(2)	55(1)
F(1)	3279(13)	1116(12)	7530(12)	226(8)
F(2)	4417(9)	139(12)	8647(8)	171(6)
F(3)	2884(12)	−1291(16)	8521(16)	292(11)
F(4)	1772(10)	−365(11)	7410(10)	193(6)
F(5)	2322(15)	545(21)	8697(13)	307(12)
F(6)	3855(14)	−760(16)	7385(12)	246(9)
N(10)	2797(12)	742(13)	4613(7)	96(5)
C(10)	3645(12)	1331(12)	4913(9)	71(5)
C(11)	4762(13)	2117(16)	5325(12)	118(8)

[a] Equivalent isotropic U defined as one-third of the trace of the orthogonalized U_{ij} tensor.

(15) Gulliver, D. J.; Hope, E. G.; Levason, W.; Murray, S. G.; Potter, D. M.; Marshall, G. L. *J. Chem. Soc., Perkin Trans. 2* **1984**, 429.

Table 3. Atomic Coordinates ($\times 10^4$) and Equivalent Isotropic Displacement Coefficients ($Å^2 \times 10^3$) for $[Pt([16]aneSe_4)]^{2+}$

	x	*y*	*z*	*U*(eq)[a]
Pt	0	0	0	40(1)
Se(1)	−804(4)	1810(2)	−966(2)	50(2)
C(2)	−1309(32)	3045(22)	−91(15)	61(7)
C(3)	−256(30)	3560(20)	627(15)	57(8)
C(4)	300(31)	2668(20)	1437(14)	54(7)
Se(5)	1452(4)	1389(2)	1044(2)	54(2)
C(6)	1711(34)	532(22)	2281(14)	60(8)
C(7)	2711(35)	−465(24)	2361(16)	70(9)
C(8)	2576(34)	−1300(22)	1485(17)	66(8)
P(1)	3138(17)	−49(8)	8040(5)	75(7)
F(1)	3352(30)	1092(26)	7458(24)	214(20)
F(2)	4359(37)	192(27)	8701(19)	235(22)
F(3)	2817(31)	−1136(35)	8576(28)	263(24)
F(4)	1882(40)	−339(24)	7354(25)	231(24)
F(5)	2180(35)	759(33)	8479(24)	210(22)
F(6)	3970(35)	−839(30)	7497(25)	217(22)
N(10)	2750(33)	766(25)	4617(17)	105(9)
C(10)	3718(50)	1352(32)	4940(22)	90(11)
C(11)	4729(41)	2148(36)	5291(22)	139(16)

[a] Equivalent isotropic *U* defined as one-third of the trace of the orthogonalized $\mathbf{U}_{ij}$ tensor.

Table 4. Selected Bond Lengths (Å), Bond Angles (deg), and Torsion Angles for $[Pd([16]aneSe_4)]^{2+}$ with Esd's in Parentheses

Pd−Se(1)	2.435(2)	Pd−Se(5)	2.428(1)
Pd−Se(1A)	2.435(2)	Pd−Se(5A)	2.428(1)
Se(1)−C(2)	1.955(10)	Se(1)−C(8A)	1.950(9)
C(2)−C(3)	1.498(13)	C(3)−C(4)	1.502(13)
C(4)−Se(5)	1.958(10)	Se(5)−C(6)	1.947(10)
C(6)−C(7)	1.550(16)	C(7)−C(8)	1.501(14)
C(8)−Se(1A)	1.950(9)	P(1)−F(1)	1.493(14)
P(1)−F(2)	1.504(9)	P(1)−F(3)	1.480(19)
P(1)−F(4)	1.536(11)	P(1)−F(5)	1.417(19)
P(1)−F(6)	1.503(17)	N(10)−C(10)	1.102(17)
C(10)−C(11)	1.465(19)		

Se(1)−Pd−Se(5)	88.9(1)	Se(1)−Pd−Se(1A)	180.0(1)
Se(5)−Pd−Se(1A)	91.1(1)	Se(1)−Pd−Se(5A)	91.1(1)
Se(5)−Pd−Se(5A)	180.0(1)	Se(1A)−Pd−Se(5A)	88.9(1)
Pd−Se(1)−C(2)	106.6(3)	Pd−Se(1)−C(8A)	103.2(3)
C(2)−Se(1)−C(8A)	93.8(4)	Se(1)−C(2)−C(3)	114.8(7)
C(2)−C(3)−C(4)	115.0(8)	C(3)−C(4)−Se(5)	114.1(7)
Pd−Se(5)−C(4)	104.8(3)	Pd−Se(5)−C(6)	104.0(3)
C(4)−Se(5)−C(6)	93.3(4)	Se(5)−C(6)−C(7)	110.8(7)
C(6)−C(7)−C(8)	116.3(8)	C(7)−C(8)−Se(1A)	112.7(7)
F(1)−P(1)−F(2)	88.3(7)	F(1)−P(1)−F(3)	176.0(10)
F(2)−P(1)−F(3)	93.5(7)	F(1)−P(1)−F(4)	92.7(7)
F(2)−P(1)−F(4)	175.1(7)	F(3)−P(1)−F(4)	85.3(8)
F(1)−P(1)−F(5)	92.4(11)	F(2)−P(1)−F(5)	96.9(8)
F(3)−P(1)−F(5)	90.9(12)	F(4)−P(1)−F(5)	87.8(8)
F(1)−P(1)−F(6)	89.2(9)	F(2)−P(1)−F(6)	84.3(7)
F(3)−P(1)−F(6)	87.5(10)	F(4)−P(1)−F(6)	91.0(7)
F(5)−P(1)−F(6)	178.1(11)	N(10)−C(10)−C(11)	179.0(15)

C(8A)−Se(1)−C(2)−C(3)	170.6
Se(1)−C(2)−C(3)−C(4)	−73.5
C(2)−C(3)−C(4)−Se(5)	76.6
C(6)−Se(5)−C(4)−C(3)	−175.8
C(4)−Se(5)−C(6)−C(7)	−173.1
C(8)−C(7)−C(6)−Se(5)	−43.9
Se(1A)−C(8)−C(7)−C(6)	−42.6
C(7)−C(8)−Se(1A)−C(2A)	−170.8
C(3A)−C(2A)−Se(1A)−C(8)	−170.6
C(4A)−C(3A)−C(2A)−Se(1A)	73.5
Se(5A)−C(4A)−C(3A)−C(2A)	−76.6
C(3A)−C(4A)−Se(5A)−C(6A)	175.8
C(7A)−C(6A)−Se(5A)−C(4A)	173.1
Se(5A)−C(6A)−C(7A)−C(8A)	43.9
C(2)−Se(1)−C(8A)−C(7A)	170.8
C(6A)−C(7A)−C(8A)−Se(1)	42.6

(b) Synthesis of $[Pt([16]aneSe_4)](PF_6)_2$. Method (a) was followed, using $PtCl_2$ (24 mg, 0.09 mmol), [16]aneSe$_4$ (43 mg, 0.09 mmol), and $TlPF_6$ (62 mg, 0.18 mmol). The product was isolated as colorless crystals. Anal. Calcd for $C_{12}H_{24}F_{12}P_2PtSe_4$: C, 14.9; H, 2.50. Found: C, 14.7; H, 2.26. FAB mass spectrum (3-NOBA matrix) *m/z*: found M^+ = 825, 679; calculated for $[^{195}Pt([16]aneSe_4)PF_6]^+$ M^+ = 826, $[^{195}Pt([16]aneSe_4)]^+$ M^+ = 681. UV/visible spectrum (MeCN solution): λ_{max} = 253 nm (ϵ_{max} = 23 570 dm^3 mol^{-1} cm^{-1}), 341 (817). $^{13}C\{^1H\}$ NMR spectrum (90.53 MHz, $(CD_3)_2CO$, 300 K): 33.1, 33.0, 32.9, 31.7, 31.0, 27.5, 27.3, 23.9, 23.5 ppm. $^{77}Se\{^1H\}$ NMR spectrum: (68.68 MHz, CD_3CN, 300 K) 187, 147 ppm; (Me_2CO, 185 K): 188 ppm. ^{195}Pt NMR spectrum: (77.4 MHz, MeCN, 300 K) −4568, −4587, −4676 ppm; (Me_2CO, 280 K) −4594, −4614, −4594 ppm; (Me_2CO, 210 K) −4750 ppm ($w_{1/2}$ *ca.* 240 Hz). IR spectrum (Nujol mull): 2724 m, 1299 m, 1266 w, 1226 w, 1154 w, 1076 w, 995 w, 839 vs, b, 557 vs cm^{-1}.

Table 5. Selected Bond Lengths (Å), Angles (deg), and Torsion Angles (deg) for $[Pt([16]aneSe_4)]^{2+}$ with Esd's in Parentheses

Pt−Se(1)	2.420(3)	Pt−Se(5)	2.417(3)
Pt−Se(1A)	2.420(3)	Pt−Se(5A)	2.417(3)
Se(1)−C(2)	1.921(25)	Se(1)−C(8A)	1.919(32)
C(2)−C(3)	1.460(35)	C(3)−C(4)	1.521(30)
C(4)−Se(5)	1.931(27)	Se(5)−C(6)	1.943(21)
C(6)−C(7)	1.462(43)	C(7)−C(8)	1.504(33)
C(8)−Se(1A)	1.919(32)	P(1)−F(1)	1.496(32)
P(1)−F(2)	1.456(35)	P(1)−F(3)	1.442(40)
P(1)−F(4)	1.511(38)	P(1)−F(5)	1.502(39)
P(1)−F(6)	1.485(38)	N(10)−C(10)	1.195(52)
C(10)−C(11)	1.365(57)		

Se(1)−Pt−Se(5)	88.8(1)	Se(1)−Pt−Se(1A)	180.0(1)
Se(5)−Pt−Se(1A)	91.2(1)	Se(1)−Pt−Se(5A)	91.2(1)
Se(5)−Pt−Se(5A)	180.0(1)	Se(1A)−Pt−Se(5A)	88.8(1)
Pt−Se(1)−C(2)	106.5(7)	Pt−Se(1)−C(8A)	101.9(7)
C(2)−Se(1)−C(8A)	96.1(12)	Se(1)−C(2)−C(3)	117.1(22)
C(2)−C(3)−C(4)	115.7(19)	C(3)−C(4)−Se(5)	113.3(17)
Pt−Se(5)−C(4)	105.0(8)	Pt−Se(5)−C(6)	104.1(8)
C(4)−Se(5)−C(6)	94.4(11)	Se(5)−C(6)−C(7)	113.8(19)
C(6)−C(7)−C(8)	112.9(22)	C(7)−C(8)−Se(1A)	116.0(24)
F(1)−P(1)−F(2)	91.3(18)	F(1)−P(1)−F(3)	175.3(21)
F(2)−P(1)−F(3)	92.8(18)	F(1)−P(1)−F(4)	89.8(17)
F(2)−P(1)−F(4)	178.3(18)	F(3)−P(1)−F(4)	86.1(19)
F(1)−P(1)−F(5)	85.5(19)	F(2)−P(1)−F(5)	100.7(19)
F(3)−P(1)−F(5)	91.5(22)	F(4)−P(1)−F(5)	80.6(20)
F(1)−P(1)−F(6)	91.9(19)	F(2)−P(1)−F(6)	85.8(20)
F(3)−P(1)−F(6)	90.6(21)	F(4)−P(1)−F(6)	93.0(19)
F(5)−P(1)−F(6)	173.1(19)	N(10)−C(10)−C(11)	173.1(40)

C(8A)−Se(1)−C(2)−C(3)	168.8
Se(1)−C(2)−C(3)−C(4)	−72.0
C(2)−C(3)−C(4)−Se(5)	74.8
C(6)−Se(5)−C(4)−C(3)	−176.1
C(4)−Se(5)−C(6)−C(7)	−172.2
C(8)−C(7)−C(6)−Se(5)	−45.1
Se(1A)−C(8)−C(7)−C(6)	−43.5
C(2A)−Se(1A)−C(8)−C(7)	−169.5
C(3A)−C(2A)−Se(1A)−C(8)	−168.8
C(4A)−C(3A)−C(2A)−Se(1A)	72.0
Se(5A)−C(4A)−C(3A)−C(2A)	−74.8
C(3A)−C(4A)−Se(5A)−C(6A)	176.1
C(7A)−C(6A)−Se(5A)−C(4A)	172.2
Se(5A)−C(6A)−C(7A)−C(8A)	45.1
C(7A)−C(8A)−Se(1)−C(2)	169.5
C(6A)−C(7A)−C(8A)−Se(1)	43.5

(c) Single-Crystal X-ray Analyses. Single crystals of both complexes were obtained by slow diffusion of Et_2O into MeCN solutions of the complexes. The selected crystals were mounted onto quartz glass fibers with epoxy resin and coated with epoxy to inhibit desolvation and crystal decomposition during data collection. The accurate unit cell parameters were obtained by a least-squares analysis of 18−25 centered reflections. Data for both were collected on a Siemens P4/PC diffractometer using graphite-monochromated Mo-K_α radiation. A summary of the crystallographic data and data collection and refinement parameters is given in Table 1. Two standard reflections were monitored every 50 reflections. For the Pd(II) complex, these reflections showed no significant variation over the data collection whereas,

(16) SHELXTL version 4.2, Siemens X-ray Analytical Instruments, 1991.

for the Pt(II) complex, there was a progressive reduction in the intensity of the reflections and the collection was terminated when the count rate had fallen to *ca.* 30% of the original. The data sets were corrected for absorption, and both structures were solved by direct methods. For the Pd(II) structure, all non-H atoms were refined anisotropically; for the Pt(II) complex, because of the reduced data set, only the Pt, Se, P, and F atoms were refined anisotropically. The H atoms, with the exception of those of the MeCN solvent (which were located from a ΔF map), were placed in calculated positions and allowed to ride on their parent carbon atoms with isotropic thermal parameters $U(H) = 1.2U_{eq}(C)$. In both structures the PF_6^- anions are disordered and consequently display high thermal anisotropy; alternative partial occupancy locations for the F atoms could not be identified.

As the truncated data set for the Pt(II) complex (before the crystal decomposed) confirmed the structure to be isomorphous with that of the Pd(II) complex, including, as well, the position and orientation of the MeCN solvent molecules, a further data collection with a new crystal was not deemed necessary.

Fractional atomic coordinates and equivalent isotropic displacement coefficients for the Pd(II) and Pt(II) complexes are given in Tables 2 and 3. Selected bond lengths, angles, and torsion angles are given in Tables 4 and 5.

(d) Synthesis of $[Pd(MeSeCH_2CH_2CH_2SeMe)_2](PF_6)_2$. Method (a) was followed, using $PdCl_2$ (39 mg, 0.22 mmol), $MeSeCH_2CH_2CH_2SeMe$ (101 mg, 0.439 mmol), and $TlPF_6$ (153 mg, 0.438 mmol). The product was isolated as a yellow solid. Anal. Calcd for $C_{10}H_{24}F_{12}P_2PdSe_4$: C, 14.0; H, 2.8. Found: C, 13.8; H, 1.81. FAB mass spectrum (3-NOBA matrix), *m/z*: found $M^+ = 713$, 568; calculated for $[^{106}Pd(MeSeCH_2CH_2CH_2SeMe)_2PF_6]^+$ $M^+ = 711$, $[^{106}Pd(MeSeCH_2CH_2CH_2SeMe)_2]^+$ $M^+ = 566$. UV/visible spectrum (MeCN solution): $\lambda_{max} = 321$ nm ($\epsilon_{mol} = 18\,800$ dm^3 mol^{-1} cm^{-1}), 361 sh (*ca.* 12 650). ^1H NMR spectrum (300 MHz, CD_3CN, 300 K): 3.0 ($SeCH_2$, 8H), 2.5 (Me, 12H), 2.2 ppm ($CH_2CH_2CH_2$, 4H). $^{13}C\{^1H\}$ NMR spectrum (90.53 MHz, CD_3CN, 300 K): 29.6 ($SeCH_2$, 4C), 24.6 (Me, 4C), 12.4 ppm ($CH_2CH_2CH_2$, 2C). ^{77}Se NMR spectrum (68.68 MHz, CD_3CN): (300 K) 132 ppm; (255 K) 135, 132, 128, 118 ppm; (200 K) 124 ppm. IR spectrum (Nujol mull): 2723 m, 1413 m, 1295 m, 1278 m, 1257 m, 1172 m, 1009 w, 926 m, 834 vs, b, 556 vs cm^{-1}.

(e) Synthesis of $[Pt(MeSeCH_2CH_2CH_2SeMe)_2](PF_6)_2$. Method (a) was followed, using $PtCl_2$ (184 mg, 0.69 mmol), $MeSeCH_2CH_2CH_2SeMe$ (320 mg, 1.4 mmol), and $TlPF_6$ (485 mg, 1.4 mmol). The product was isolated as a pale yellow solid (37%). Anal. Calcd for $C_{10}H_{24}F_{12}P_2PtSe_4$: C, 12.7; H, 2.5. Found: C, 12.8; H, 1.80. UV/visible spectrum (MeCN solution): $\lambda_{max} = 245$ nm ($\epsilon_{mol} = 17\,400$ dm^3 mol^{-1} cm^{-1}), 261 sh (*ca.* 12 900), 284 sh (*ca.* 7600). ^1H NMR spectrum (300 MHz, CD_3CN, 300 K): 3.3 ($SeCH_2$, 8H), 2.6 (Me, 12H), 2.2 ppm ($CH_2CH_2CH_2$, 4H). $^{13}C\{^1H\}$ NMR spectrum (90.53 MHz, CD_3CN, 300 K): 30.7, 30.1, 24.6, 13.7, 12.8 ppm. ^{77}Se NMR spectrum (68.68 MHz, CD_3CN, 300 K): 128.3, 127.3 ppm. ^{195}Pt NMR spectrum (77.4 MHz, CD_3CN): (300 K) −4677 (major), −4663, −4657 ppm; (185 K) −4676 (major), −4663, −4653 ppm. IR spectrum (Nujol mull): 2724 m, 1413 m, 1294 m, 1278 m, 1259 m, 1177 w, 1010 m, 927 m, 835 vs, b, 557 vs, 442 w cm^{-1}.

Acknowledgment. We thank Johnson Matthey plc for loans of platinum metal salts.

Supplementary Material Available: Tables of anisotropic thermal parameters and hydrogen positions for $[M([16]aneSe_4)](PF_6)_2 \cdot 2MeCN$, M = Pd, Pt (2 pages). Ordering information is given on any current masthead page.

IC940455N